ACS POLYMERS Au
AN OPEN ACCESS JOURNAL OF THE AMERICAN CHEMICAL SOCIETY

pubs.acs.org/polymerau

Article

Decoupling of Glassy Dynamics from Viscosity in Thin Supported Poly(*n*-butyl methacrylate) Films

Mithun Chowdhury,* Xavier Monnier, Daniele Cangialosi, and Rodney D. Priestley

Cite This: *ACS Polym. Au* 2022, 2, 333−340

Read Online

ACCESS | Metrics & More | Article Recommendations

ABSTRACT: We utilized fast scanning calorimetry to characterize the glass transition temperature (T_g) and intrinsic molecular mobility of low-molecular-weight poly(*n*-butyl methacrylate) thin films of varying thicknesses. We found that the T_g and intrinsic molecular mobility were coupled, showing no film thickness-dependent variation. We further employed a unique noncontact capillary nanoshearing technique to directly probe layer-resolved gradients in the rheological response of these films. We found that layer-resolved shear mobility was enhanced with a reduction in film thickness, whereas the effective viscosity decreased. Our results highlight the importance of polymer−substrate attractive interactions and free surface-promoted enhanced mobility, establishing a competitive nanoconfinement effect in poly(*n*-butyl methacrylate) thin films. Moreover, the findings indicate a decoupling in the thickness-dependent variation of T_g and intrinsic molecular mobility with the mechanical responses (shear mobility and effective viscosity).

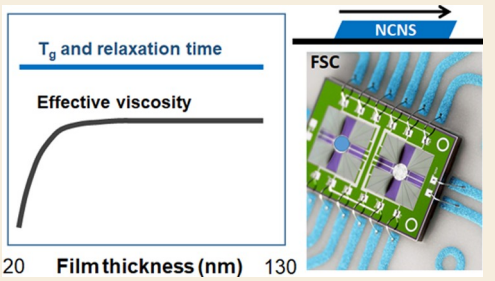

KEYWORDS: *polymer thin film, glass transition, viscosity, shear mobility, confinement, molecular mobility*

INTRODUCTION

Since its first perception nearly three decades ago,[1] it has been widely accepted that geometrical confinement may alter the glass transition temperature (T_g) of thin glassy polymer films with respect to the bulk, as a result of perturbations induced by interfacial interactions at the substrate and the presence of a free surface.[2−11] The effect of competing interfaces further led to several important findings, such as interfacial gradients in T_g,[6] viscosity,[12−14] shear mobility,[13] and structural relaxation.[10,15] Moreover, recent important developments show that interfacial mobility gradients can lead to rubbery surfaces on top of polymer glasses[11] and that the progressive irreversible adsorption of polymers at substrate can erase film thickness-dependent T_g reductions.[3] While such investigations are rooted in deep intellectual interest to better understand the glass transition of polymers under geometrical confinement, it has also great importance for what concerns the knowledge for fabrication, processing, and storing of coatings, devices, and structures where polymers are exposed to nanoscale interfaces shared with nonpolymeric substances.[9,16]

Molecular mobility in confined polymers related to the glass transition is often loosely defined. It can be a measure of relaxation processes, connected to the segmental-level motion of polymer chains. In this case, spontaneous fluctuations are considered, which can only be characterized if small perturbations, such as small temperature jumps, are applied to the system. This can be further connected to diffusion and viscosity.[8,17] From the dynamic picture, the glass transition temperature is defined as the temperature at which the relaxation time attains a value normally between 1 and 1000 s.[17−19] On the contrary, the glass transition can be seen from the viewpoint of the transformation of a melt into a glass, also addressed as vitrification. This is generally marked by a discontinuous change in specific heat at T_g, resulting in a change in the temperature dependence of enthalpy, specific volume, entropy, and density, further affecting material properties like stiffness.[5,10,13,18] Despite the conceptual difference, there exist numerous attempts to connect the film thickness-dependent T_g to molecular mobility, diffusion, viscosity, and stiffness.[8,17] However, it appears that building such a nexus in thin films where each of the properties correlate with a simple meaningful interdependence with T_g is nonexistent. There exist many anomalous phenomenological observations, such as decoupling between segmental dynamics and T_g[17,20,21] and anomalous broadening of T_g.[22−24] Decoupling of dynamics in glass formers is a well-known phenomenon;[8,17,25] in fact, the typical disparity in the time scales of α-relaxation time (responsible for T_g) and chain diffusion for long-chain polymers (involving reptation, the time

Received: March 26, 2022
Revised: May 31, 2022
Accepted: June 13, 2022
Published: June 30, 2022

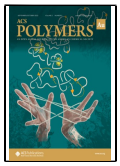

https://doi.org/10.1021/acspolymersau.2c00010
ACS Polym. Au 2022, 2, 333−340

scale of which is in general several orders magnitude larger than the α-relaxation time) illustrates decoupling of local vs global chain dynamics.[17,18,26]

Decoupling of dynamics takes an interesting yet debatable outlook when discussed within the context of conflicting thickness-dependent glass transition dynamics of glassy thin films.[8,14,17,20,25,27,28] Several dielectric spectroscopy investigations confirmed the presence of bulklike segmental dynamics for polymers even under severe confinement.[20,21] This led Cangialosi and co-workers to put forward an alternate explanation to the variation of T_g via the free volume hole diffusion model;[17,29,30] specifically, confined films having larger ratios of the free surface to volume facilitate greater free volume holes diffusion to the surface for annihilation. In another way, enhanced free surface mobility in polymer films assists the release of free volume holes.[30] This implies that equilibrium is maintained at lower temperatures, thus resulting in depressed T_g. Importantly, the free surface effect can be erased[3] by putting the film in contact with an adsorbing interface, resulting in an insurmountable barrier to free volume release.[29−31]

Decoupling of viscosity from T_g in thin glassy polymer films has been frequently observed. Bodiguel and Fretigny reported that the reduction in viscosity in thin polystyrene films atop liquid substrate was not coupled with the reduction in T_g shown by supported polystyrene thin films.[32] Very recently, Xu et al. showed evidence of the decoupled role of film thickness and polymer−substrate interfacial effects in poly(methyl methacrylate) (PMMA) thin films.[28] As per their findings, thin films with dissimilar thicknesses and interfacial properties can have the same T_g but very different thermal expansivity, thus signifying interfacial interactions as the dominant contributor over film thickness to decide the T_g.[28] This observation aligns with an earlier view of Vogt and co-workers,[33] where an increase in alkyl group size in poly(alkyl methacrylates) led to more prominent decoupling between T_g and the coefficient of thermal expansion. Tsui and co-workers observed a thickness-independent diffusion coefficient and T_g in poly(isobutyl methacrylate) (PIBMA) thin films, while the effective viscosity decreased systematically below the 50 nm film thickness.[14] If we envisage that diffusion and viscosity in thin films depend on similar kinds of transport phenomena involving local segmental friction and slippage, this is rather surprising. These observations surely resurface recent important questions: "Why we need to look beyond the glass transition temperature to characterize the dynamics of thin supported polymer films?"[34] and "When does a glass transition temperature not signify a glass transition?"[35]

In the present work, we show a scenario of thickness-invariant T_g and intrinsic molecular mobility in low-molecular-weight poly(n-butyl methacrylate) (PNBMA) films of various thicknesses, measured through fast scanning calorimetry (FSC). Further, we apply the film depth-resolved NCNS (noncontact capillary nanoshearing) technique by tracking a step-edge profile in the film under gas flow-induced shear deformation to find the shear mobility and effective viscosity.[13] We find that shear mobility inside a film increases from the bulk to the free surface, which further leads to a reduction in effective viscosity upon approaching the film surface. Comparing films of different thicknesses after certain durations of NCNS, we found that shear mobility enhances with decreasing film thickness, which is most prominent for the thinnest film. This corresponds to a similar extent of reduction in effective viscosity upon a decrease in film thickness, supporting earlier work on PIBMA.[14] Overall, our results suggest that polymer−substrate attractive interactions and free-surface-promoted enhanced mobility impart a competitive nanoconfinement effects on poly(n-butyl methacrylate) thin films. In summary, we observed a decoupling between the thickness dependence of glassy dynamics (T_g and intrinsic molecular mobility) and mechanical response (shear mobility and effective viscosity) in PNBMA thin films.

MATERIALS AND METHODS

Poly(n-butyl methacrylate) (PNBMA, M_w = 2.8 kD, M_w/M_n < 1.15, PSS Polymer Standards Service GmbH, Germany) solutions in toluene at varying concentrations were spin-coated to obtain films of variable thicknesses: 22, 45, 90, and 125 nm. In NCNS experiments, we used as-received Si/SiO_x (100) wafer as the substrate for spin-coating, whereas fast scanning calorimetry (FSC) experiments were carried out with a Flash DSC1, Mettler-Toledo, under ∼20 ml/min nitrogen flux equipped with an intracooler allowing temperature control between −90 and 450 °C.[36] The Flash DSC1 relies on chip technology, where micron-thick membranes are employed, thereby drastically reducing the overall mass setup with respect to standard calorimetry. Sample masses were reduced from sub-micrograms to nanograms. This kind of setup permits heating/cooling rates ranging from 0.1 to several thousand K/s. Samples were spin-coated on the backside of conditioned UFS-1 sensors (Mettler-Toledo).[37] The sensor is made of two identical squared membranes, whose backside is covered by silicon oxide, deposited on top of an aluminum core. Hence, the portion of the sensor in touch with the polymer is SiO_x. Characterization of the intrinsic molecular mobility was performed by determining the complex specific heat capacity, $C_p^*(\omega)$, through the step response analysis.[27,38,39] The thermal protocol for such analysis consists of a temperature increase of 2 K followed by isotherms of durations 0.1 and 0.5 s during which the instantaneous heat flow rate HF(t) is recorded. HF(t) and cooling rate $\beta_c(t)$ are Fourier-transformed to determine the complex specific heat

$$C_p^*(\omega) = \frac{\int_0^{t_p} \mathrm{HF}(t)\exp(-i\omega t)\mathrm{d}t}{\int_0^{t_p} \beta_c(t)\exp(-i\omega t)\mathrm{d}t} \quad (1)$$

Using this transformation, the complex specific heat is obtained at the base frequency and higher harmonics: $\omega = \frac{2\pi k}{t_p}$, where k is an integer and t_p is the duration of the temperature step plus the isotherm. We explored the frequency range within 2−100 Hz by changing t_p via accessing higher harmonics. The 2 K temperature jump assures linearity of the measurement, as temperature fluctuations are generally larger than 2 K, and thereby, higher-order contributions to C_p are generally negligible. Thus, intrinsic molecular mobility is accessed by this method. This procedure can show complex specific heat: $C_p^* = C_p' + iC_p''$. Using it the reversing specific heat, $C_{p,rev} = (C_p'^2 + iC_p''^2)^{1/2}$was obtained. This is different from the total specific heat C_p, as it does not contain non-reversing contributions to the specific heat, that is, those associated with the kinetics of (de)vitrification.[27] Hence, $C_{p,rev}$ provides a baseline-corrected estimation of $C_{p,glass}$ and $C_{p,liquid}$. Moreover, $C_{p,rev}$ almost coincides with C_p', as the latter is generally at least one order of magnitude larger than C_p''.[27]

FSC experiments were also used to characterize the cooling rate-dependent fictive temperature (T_f), which provides insights into vitrification kinetics. It is worth noticing that for samples cooled and heated at the same rate, the glass T_f essentially coincides with the T_g.[40] Samples of all thicknesses were cooled at different rates between 1 and 1000 K/s and immediately heated at 5000 K/s for data recording. To obtain T_f, heating scans were analyzed via the Moynihan method,[41] which mathematically reads

$$\int_{T^*}^{T_f} (C_{p,\mathrm{melt}} - C_{p,\mathrm{glass}})\mathrm{d}T_f = \int_{T^*}^{T'} (C_p - C_{p,\mathrm{glass}})\mathrm{d}T \quad (2)$$

https://doi.org/10.1021/acspolymersau.2c00010
ACS Polym. Au 2022, 2, 333−340

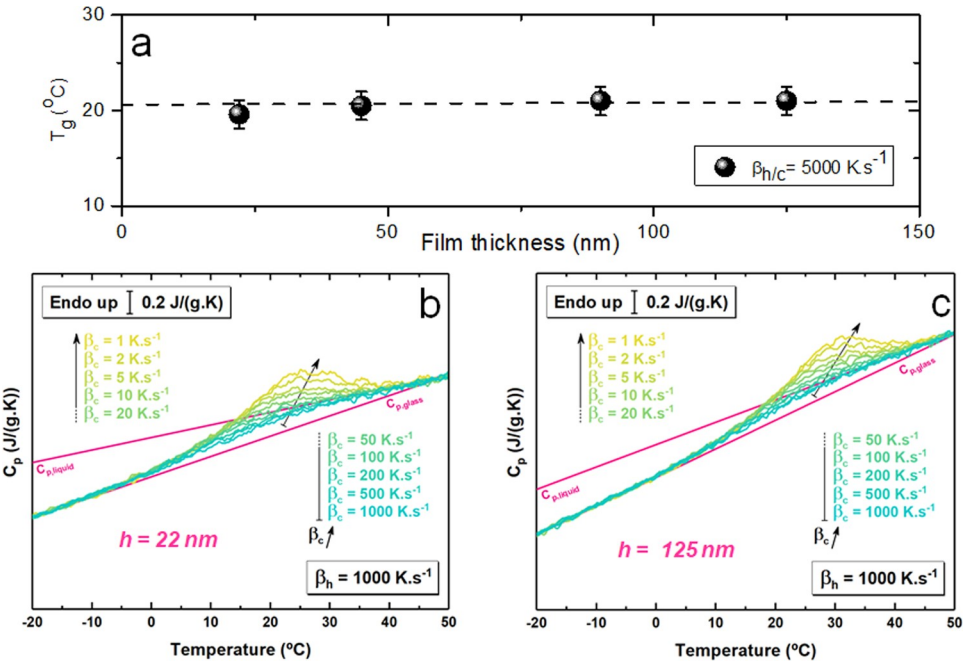

Figure 1. Fast scanning calorimetry (FSC) studies of PNBMA 2.8 kD films. (a) Glass transition temperature (T_g) for all different film thicknesses taken during the second heating of samples, where the heating and cooling rate is $\beta_{h/c}$ = 5000 K·s^{-1}. We found T_g (22 nm) = 19.5 °C, T_g (45 nm) = 20.5 °C, T_g (90 nm) = 21 °C, and T_g (125 nm) = 21 °C. The error bar for repeated measurements including nominally similar samples is 1.5 °C. (b−c) Specific heat versus temperature upon heating at 1000 K·s^{-1} after cooling at the indicated rates for the thinnest ((b) h = 22 nm) and thickest ((c) h = 125 nm) films studied.

where C_p, $C_{p,melt}$, and $C_{p,glass}$ are the specific heat resulting from the heating scan, melt, and glass, respectively. Here, T' is a temperature above the transition region at which the heat capacity is equal to the equilibrium melt value, $C_{p,melt}$, and T^* is a temperature well below the glass transition region., where C_p equals $C_{p,glass}$.

The basis of the NCNS method relies on measuring polymer deformation under shear induced by the gas flow. It is a modified version of the blow-off method classically used to determine shear mobility of boundary liquids over a surface,[42−44] here with added temperature controlling measurement. As detailed in our previous work on NCNS, thin PNBMA films supported atop a solid Si/SiO_x substrate are placed inside a microchannel at 45 °C (ca. $T_{g,bulk}$ + 24 °C). Microchannel dimensions ensure laminar gas (dry pure nitrogen) flow inside the flow cell.[43,44] Gas source and flow cell are both capable of temperature control up to 130 °C. Gas flow imparts shear stress on the film which can be calculated via the Hagen−Poiseuille relationship[13,43] as $\sigma = \Delta Pd/2L$, where d and L are geometric parameters of the cell, and pressure drop ΔP can be monitored through a pressure gauge. Throughout our experiments, we use shear stress σ = 174 Pa, with the following geometrical parameters of flow cell (channel dimensions: d = 60 μm, L = 19 mm) and pressure drop ΔP = 16 psi. A detailed description of the flow cell and apparatus assembly can be found in our earlier work introducing the NCNS technique in detail.[13]

We consider a mechanically cut sharp step-edge in each of our PNBMA films to shear using the above protocol, as response time-dependent deformation of the film can be followed by monitoring the time evolution of the film (step-edge) profile via atomic force microscopy (AFM). It enables calculating viscoelastic responses by a layer-by-layer approach. Typically, areas of 10 × 50 mm^2 in the topographic images were analyzed to obtain the data of the film profile. The raw data of the film profile acquired from AFM images were smoothed by fitting to second-order polynomials prior to computing shear mobility, as explained later in the Results and Discussion section. The obtained fit functions were considered to smoothly interpolate over the data range with desired increments, from the substrate to free surface (or from the free surface to substrate) along the film thickness that was subsequently utilized for layer-by-layer analysis to calculate the shear mobility and effective viscosity. The layer-average shear mobility was computed taking the mean of shear data considering the entire range of film thickness undergoing NCNS, termed mean shear mobility. We consider that any tilt (ΔX) in NCNS step-edge (see Figure 4) is solely due to the shear stress imposed by the gas flow and clearly disentangle the role of NCNS from the possible associated processes, e.g., capillary leveling[45] and dewetting,[46] as detailed in our earlier work.[13]

RESULTS AND DISCUSSION

Determination of T_g and T_f

T_g's of all films have been measured while heating each of the samples at 5000 K s^{-1}. To remove the preparation-induced nonequilibrium in polymer chain conformations,[46,47] second heating cycles have been considered, after initial heating and cooling cycles (both at 5000 K s^{-1}). We found that T_g values, taken as the temperature corresponding to the midpoint of the specific heat step for all of the film thicknesses, are nearly identical at ca. 21 °C (see Figure 1a). This is comparable to the T_g of the bulk polymer. Invariant global-T_g with the film thickness of poly(butylmethacrylates) atop Si/SiO_x has been reported earlier.[14,33,48] Priestley et al. showed a 6 °C decrease in the local-T_g at the free surface on a 14 nm thick fluorescently labeled PIBMA layer, while that at the substrate surface was enhanced by 5 °C.[48] As per the current understanding, substrate effects based on attractive interactions via hydrogen bonding between the polymer and silica surface may result in an increase or decrease in T_g depending on the packing frustration in the polymer film.[49] At the immediate proximity of the substrate, even the presence of immobilized polymer fraction cannot avoid the generation of packing frustration penetrating inside the core of the film.[50] In such cases, packing frustration acts as the source of free volume and induces the same effect on confinement imposed by free

https://doi.org/10.1021/acspolymersau.2c00010
ACS Polym. Au 2022, 2, 333−340

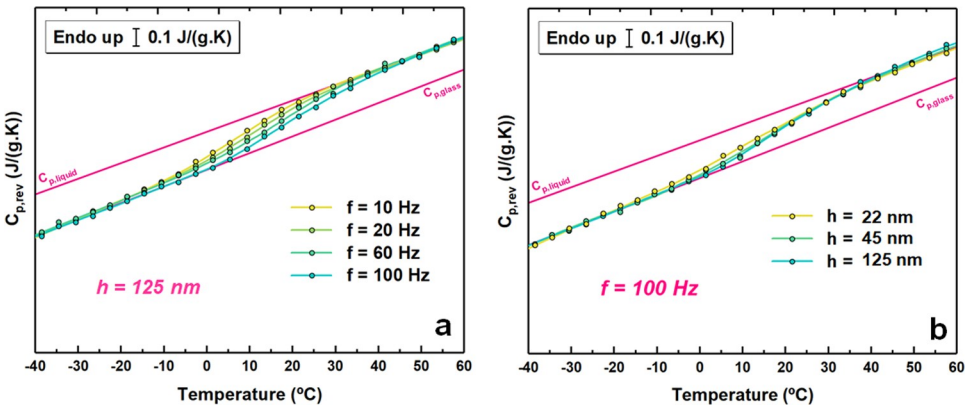

Figure 2. Reversing specific heat ($C_{p,rev}$) obtained from step response analysis versus temperature (a) as a function of frequency on a film with thickness h = 125 nm and (b) varying film thicknesses at a fixed frequency of 100 Hz.

surfaces imparting some enhanced dynamics, leading to a decrease in T_g. Altogether, these considerations would anticipate a distribution of T_g's in the film.[48]

A more comprehensive characterization of the vitrification behavior is obtained from the cooling rate and thickness-dependent T_f. Figure 1b,c shows the specific heat scans of h = 22 and 125 nm films, respectively, obtained by FSC upon heating at 1000 K·s^{-1} after cooling at the indicated rates. By decreasing the cooling rate, a gradual increase in intensity in the overshoot is evident. It appears that the cooling rate-dependent enhancement of overshoot intensity is comparable for both film thicknesses, indicating a thickness-independent scenario. Data in Figure 1b,c were analyzed via the Moynihan method, cf. eq 2, to obtain T_f. As can be observed later, T_f is independent of the film thickness over the entire investigated cooling rate range.

Determination of Intrinsic Molecular Mobility

Figure 2a depicts the frequency-dependent variation of reversing specific heat ($C_{p,rev}$) vs temperature obtained from step response analysis by FSC after Fourier transforming HF(t) and $q(t)$ for the film with h = 125 nm as a showcase. This procedure delivers the frequency-dependent complex specific heat. As expected, increasing the frequency results in a shift toward higher temperatures of $C_p' \sim C_{p,rev}$ step. Figure 2b shows the $C_{p,rev}$ at a frequency of 100 Hz for the films of thicknesses h = 22, 45, and 125 nm. From Figure 2b, we can conclude that all curves essentially collapse with each other, indicating that, at this frequency, the intrinsic molecular mobility is nearly invariant with the sample size (i.e., film thickness).

The size (film thickness) and frequency dependence on the relaxation time (τ) is shown in Figure 3, where plots of the reciprocal of τ as a function of the inverse of the temperature are shown (left axis). Here, τ is considered from the midpoint of the step of the real part of the specific heat (C_p') or equivalently the reversing specific heat ($C_{p,rev}$).[27,39] As can be observed, τ exhibits the same temperature dependence of the cooling rate (β_c, right axis) dependent T_f. For all film thicknesses, the Vogel–Fulcher–Tammann (VFT) equation $z = A + B/(T-T_0)$,[27] where z can be either log β_c^{-1}) or log τ, can be applied. We can see identical B, A, and T_0 are sufficient to fit τ and cooling-rate-dependent T_f, showing a connection between molecular mobility and vitrification behavior.[51] This result indicates complete coupling between molecular mobility and vitrification kinetics. Moreover, the results shown in Figure 3 indicate film thickness-invariant molecular dynamics throughout the whole investigated temperature range. We anticipate the reason behind this observation stands on effects resulting from PNBMA attractive interaction with the substrate, leading to irreversible adsorption of polymer chains resulting in inefficient removal of free volume from the free interface.[3,52] This finally results in the erasure of surface effects in polymer nanoconfinement leading to thickness-invariant dynamics.[3,48]

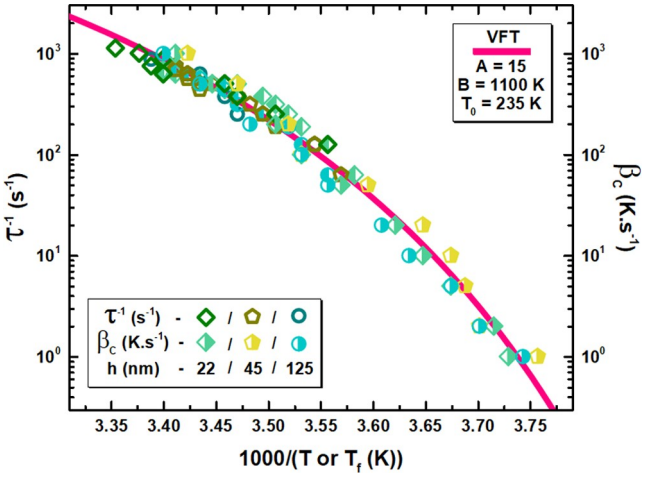

Figure 3. (Left axis) Reciprocal of the relaxation time as a function of the inverse temperature obtained considering the midpoint of the step of the reversing specific heat. Results are obtained from step response analysis on PNBMA 2.8 kD films of thickness h = 22, 45, and 125 nm at varying temperatures. (Right axis) Cooling rate-dependent T_f obtained through the Moynihan method[41] for the same films. The solid line represents the Vogel–Fulcher–Tammann fit to the reciprocal relaxation time (τ^{-1}, left axis) and cooling rate (β_c, right axis) with parameters B = 1100 K, T_0 = 235 K, and A = 15 for both τ^{-1} and for β_c.

Determination of Shear Mobility and Effective Viscosity

While our FSC studies clearly pointed out film thickness-independent T_g and intrinsic molecular mobility, NCNS can measure spatially resolved time-dependent viscoelastic response of ultrathin polymer films supported atop a substrate.[13] The idea behind utilizing NCNS for the current work is more relevant, seeing a position-dependent local-T_g reported in PIBMA films.[48] While in our present work the global-T_g of the entire film and relaxation dynamics do not show any film

https://doi.org/10.1021/acspolymersau.2c00010
ACS Polym. Au 2022, 2, 333–340

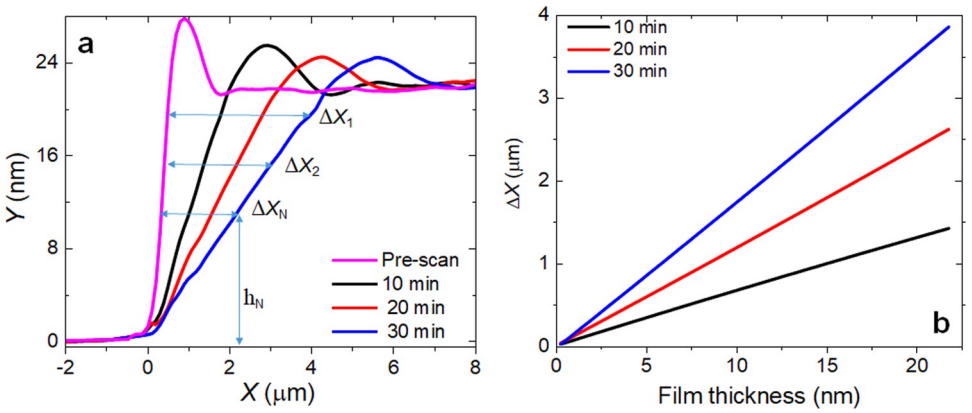

Figure 4. NCNS of PNBMA 2.8 kD, 22 nm film at 45 °C (ca. $T_{g,bulk}$ + 24 °C). Applied shear stress during NCNS σ = 174 Pa. (a) Tapping mode AFM height profiles with varying shear time in the figure legends. Rim formation at the top is due to instability on the nonwettable substrate. It is not considered a region of interest for determining the deformation (tilt) of the step-edge profile. Gradual tilting of the step-edge profile with time shows the effect of the shear stress, exhibiting a notable impact of shear as established by tilted profiles (shifted and superposed to the step-edge origin). (b) Amount of lateral deformation (tilt) in the step-edge (ΔX) upon shearing, as shown gradually in panel (a) as ΔX_1 to ΔX_N at a particular thickness h_N.[13]

thickness dependence, we put effort into exploring the capability of NCNS tool to obtain spatially resolved properties in substrate-supported PNBMA films to correlate with their intrinsic molecular mobility and T_g.

Figure 4a shows the shape of the step-edge profile changes by applied shear stress (σ = 174 Pa), showing an increment in deformation (tilt ΔX) with the duration of shearing. Shape change shows a strong dependence on depth within the film, with large deformations near the free surface decreasing toward the substrate. These observations suggest the existence of regions of enhanced and reduced mobility at the free surface and substrate interface, respectively. Figure 4b is obtained from Figure 4a, where the lateral deformation (ΔX) from the undeformed step-edge (represented as prescan in Figure 4a) has been computed in a layer-resolved way, as described in earlier work.[13]

We can calculate layer-resolved shear mobility $\chi_S(h)$ as a function of film thickness as[13,43]

$$\chi_s(h) = \frac{\Delta X(h)}{\sigma t} \tag{3}$$

where $\Delta X(h)$ is the lateral deformation at height h from the substrate, σ is the applied shear stress, and t is the time elapsed since the start of shear. Gradual deformation upon the increasing duration of shearing ensures a gradual enhancement in shear mobility. Still, to compare film thickness dependence of shear mobility, it is essential to follow shear mobility after a certain duration of application of shear stress. Figure 5 shows the layer-resolved shear mobility in PNBMA films of different thicknesses after 30 min of shearing (σ = 174 Pa).

From Figure 5, we can see monotonic thickness dependence of shear mobility, in which thinner films have higher shear mobility. Here, the thinnest h = 22 nm film shows the largest increase in shear mobility. The two intermediate film thicknesses (h = 45 and 90 nm) show comparable shear mobility, at least until ca. 25 nm distance from the substrate. The thickest film (h = 125 nm) showed further slightly lowered shear mobility. The ca. 20 nm region at the substrate's vicinity has closely comparable shear mobility for all of the films, except the thinnest h = 22 nm film. The above observation indicates the dominantly stand-out behavior of the thinnest (h = 22 nm) film. This can be explained considering

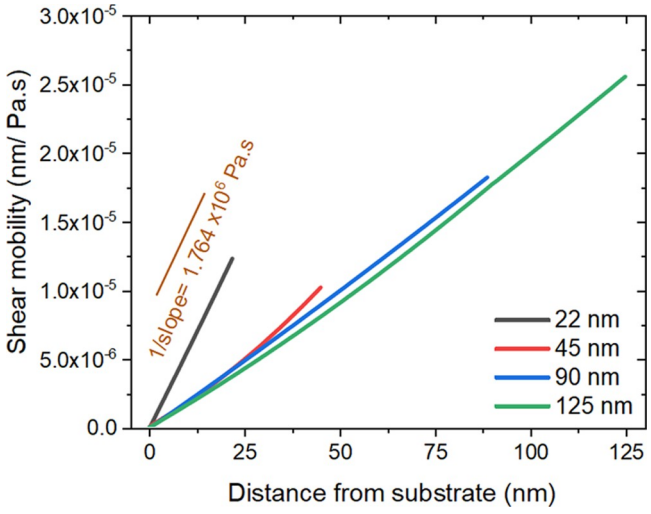

Figure 5. Shear mobility variation with distance from substrate for PNBMA 2.8 kD films (h = 22, 45, 90, and 125 nm) after 30 min of shearing, under shear stress σ = 174 Pa at 45 °C (ca. $T_{g,bulk}$ + 24 °C).; 1/slope is representing the effective viscosity for each of the film thicknesses.

the competitive contribution of the free surface effect and attractive interaction between PNBMA-Si/SiO_x.[33] The impact of substrate interaction propagates to the free surface even for the 125 nm thick film, where the shear mobility is much smaller than that of the 22 nm film. Such contributions should generally fade out for relatively thicker films due to the larger distance between the film free surface and substrate interface,[3] imparting greater response on the movement of molecules upon NCNS.[8] If we consider the free surface effect, we can say it is more pronounced in the thinnest 22 nm film, imparting enhanced intrinsic molecular mobility, one of the most acceptable views in thin confined polymer films.[1,3,4] Surprisingly, this is apparently against the thickness-independent T_g values we found in thin films that are comparable to $T_{g,bulk}$ and have comparable intrinsic molecular mobility irrespective of film thickness.

Observation of film thickness-dependent shear mobility, qualitatively, agrees with experiment[43] and molecular dynamics

https://doi.org/10.1021/acspolymersau.2c00010
ACS Polym. Au 2022, 2, 333−340

simulation[53] studies considering blow-off driven shear properties of ultrathin lubricant films as a boundary liquid on a solid substrate. A recent theoretical framework by George et al.[54] showed an inverse relationship between in-plane shear modulus and film thickness for polymer films. The provided shear modulus restricts shear mobility; we arrive at a similar conclusion qualitatively. However, interestingly, our experiments rely on the role of substrate, whereas their theoretical studies[54] considered freestanding polymer films. Indeed, this observation glorifies the free surface's role in generating gradient shear mobility across film thickness.

The effective viscosity (η_{eff}) in such films can be calculated as the inverse of slopes[13,43] in shear mobility vs film thickness plots (see Figure 5) as

$$\eta_{eff}(h) = \left[\frac{d\chi_s(h)}{dh}\right]^{-1} \quad (4)$$

We found a thickness-dependent monotonic variation of effective viscosity, which decreases upon film thickness reduction, all lying within the same order of magnitude of 10^6 Pa·s (see Figure 6). Here, the thinnest film showing the lowest viscosity (and the highest shear mobility) agrees with the film confinement assisted enhanced mobility. Still, in a larger scenario, this picture does not correlate with the observations like thickness-invariant T_g or intrinsic molecular mobility we have already shown in our experiments through FSC.

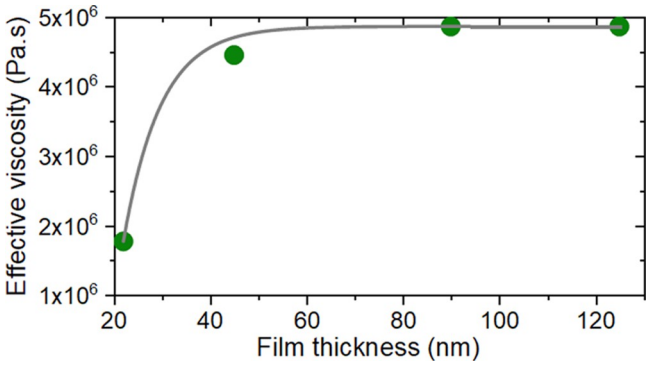

Figure 6. Effective viscosity as a function of film thickness in the PNBMA 2.8 kD film after 30 min of NCNS. Film thicknesses under consideration: h = 22, 45, 90, and 125 nm under shear stress σ = 174 Pa at 45 °C (ca. $T_{g,\,bulk}$ + 24 °C).

Viscosity studies in poly(alkyl methacrylate) thin films are relatively less. A recent report by Tsui and co-workers on PIBMA put forth a scenario of conflicting confinement where films' effective viscosity decreased upon reducing thickness below ca. 50 nm, but the in-plane dye probe diffusion coefficient and T_g did not differ from bulk.[14] It is worth mentioning that their effective viscosity was the result of calculations via a three-layer model. Also, our experimental observations on PNBMA films add a different perspective on the thickness-dependent variation of effective viscosity and shear mobility. If we compare experimental observations and the recent work by Xu et al. on PMMA thin films, there is a qualitative agreement.[28] They found that film thickness reduction led to increased thermal expansivity, whereas it contributed to an enhancement in T_g. In our present experiment, we found that film thickness reduction does not alter T_g and leads to decreased effective viscosity and enhanced shear mobility in PNBMA films. Thickness-invariant T_g and further increased tendency of decoupled thermal expansion behavior with T_g are well anticipated for PNBMA, having considerable chain stiffness, leading to diminished nanoconfinement effects.[33]

One could anticipate that a direct comparison of position-dependent local mechanical responses (shear mobility and effective viscosity) and position-dependent local-T_g would have been more appropriate for showing thickness-dependent decoupled dynamics. However, it is well known from fluorescence labeling studies that such a position-dependent variation of local-T_g in the PNBMA film is improbable, as it is less susceptible to the presence of the substrate or glassier interface.[26] As a result, in our FSC experiments, we found invariant global-T_g and intrinsic molecular mobility. This is in agreement with global-T_g measurements performed by the fluorescence labeling technique in PIBMA thin films.[14,48] It is also worth considering that position-dependent T_g would result in a broadening of glass transition, resulting from faster free surface layers and those close to the buried interface (de)vitrifying at lower and higher temperatures, respectively. Moreover, while in our NCNS experiments, effective viscosity can be represented both in terms of continuum flow- and shear-driven motion in films where local changes in thickness are only due to shear flow, it also represents a collective behavior of momentum transferred across the film under shear stress σ as $\sigma = \eta(h)\frac{dv(h)}{dh}$. Here, $v(h)$ is the velocity of the liquid in the direction of applied stress at a distance h from the liquid−solid interface and $\eta(h)$ is the dynamic viscosity of the liquid at h. Integration of the above equation over the film thickness under no-slip boundary conditions at the solid−liquid interface can give an effective viscosity representing the global film thickness.[43]

CONCLUSIONS

To conclude, our results emphasize the importance of the competitive role of the free surface and substrate interface, specifically its interaction with the polymer, perturbing intrinsic molecular mobility, glass transition, and shear response of poly(*n*-butyl methacrylate) thin films. Our results show thickness-invariant glass transition temperature and intrinsic molecular mobility. In contrast, response to shear in such films in terms of shear mobility and effective viscosity shows a film thickness-dependent scenario, implying that the competitive contribution of the free film surface and substrate interface leads to a position-dependent interdependence. Our observation of layer-resolved shear mobility and effective viscosity clearly indicates that the former enhances upon reduction of film thickness, whereas the latter decreases. This is in accordance with the well-established view of the dominant role of the film free surface in enhancing molecular mobility in confined films. This scenario along with the calorimetric observation of thickness-invariant glass transition dynamics and glass transition temperature invokes the possibility of substrate interaction perturbing molecular mobility in these films. This idea is also supported by the effective viscosity values observed in these films. Shear mobility measures how easily the molecules in a layer parallel to the free surface can be moved in the horizontal plane. In our case, it can be possibly linked to lateral transport (segmental diffusion) of polymer chains. Hence, broadly speaking, if one assumes it as a measure of generalized molecular mobility that might impact the glass

https://doi.org/10.1021/acspolymersau.2c00010
ACS Polym. Au 2022, 2, 333−340

transition of polymer films, we have clearly observed a decoupling between thickness-dependent shear mobility with intrinsic molecular mobility and glass transition temperature. Our observation underpins the fact that even a coupled dynamics of glass transition temperature and intrinsic molecular mobility with film thickness can lead to a decoupled shear mobility (and effective viscosity) response in thin poly(*n*-butyl methacrylate) films. This is another aspect of decoupling in dynamic molecular processes related to glass transition in substrate-supported confined polymer films.

AUTHOR INFORMATION

Corresponding Author

Mithun Chowdhury − *Lab of Soft Interfaces, Metallurgical Engineering and Materials Science, Indian Institute of Technology Bombay, Mumbai 400076, India; Center for Research in Nanotechnology and Science, Indian Institute of Technology Bombay, Mumbai 400076, India;* orcid.org/0000-0002-2513-6006; Email: mithunc@iitb.ac.in

Authors

Xavier Monnier − *Centro de Física de Materiales (CSIC-UPV/EHU), 20018 San Sebastián, Spain; Donostia International Physics Center, 20018 San Sebastián, Spain;* orcid.org/0000-0001-5857-7986

Daniele Cangialosi − *Centro de Física de Materiales (CSIC-UPV/EHU), 20018 San Sebastián, Spain; Donostia International Physics Center, 20018 San Sebastián, Spain*

Rodney D. Priestley − *Chemical and Biological Engineering, Princeton University, Princeton, New Jersey 08544, United States; Princeton Institute for the Science and Technology of Materials, Princeton University, Princeton, New Jersey 08540, United States;* orcid.org/0000-0001-6765-2933

Complete contact information is available at: https://pubs.acs.org/10.1021/acspolymersau.2c00010

Notes

The authors declare no competing financial interest.

ACKNOWLEDGMENTS

M.C. acknowledges support from the Science and Engineering Research Board through the Ramanujan Fellowship (Grant No. SB/S2/RJN-084/2018) and the Early Career Research Award (ECR/2018/001740) of the Department of Science and Technology, India. Additionally, support from IIT Bombay through a SEED grant (RD/0519-IRCCSH0-033) is acknowledged. R.D.P. acknowledges support from the National Science Foundation (NSF) Materials Research Science and Engineering Center Program of the Princeton Center for Complex Materials (grant numbers DMR-1420541 and DMR-2011750) and the NSF through grant number CBET-1706012. D.C. acknowledges MICINN-Spain and FEDER-UE (grant PGC2018-094548-BI00) and the Basque Government (grant IT-1175-19). The authors thank Yucheng Wang for help in data analysis at the preliminary stage of experiments and Mithun Madhusudanan for helpful comments on the manuscript.

REFERENCES

(1) Keddie, J. L.; Jones, R. A.; Cory, R. A. Size-dependent depression of the glass transition temperature in polymer films. *Europhys. Lett.* **1994**, *27*, 59.

(2) Tian, H.; Xu, Q.; Zhang, H.; Priestley, R. D.; Zuo, B. Surface dynamics of glasses. *Appl. Phys. Rev.* **2022**, *9*, No. 011316.

(3) Perez-de Eulate, N. G.; Sferrazza, M.; Cangialosi, D.; Napolitano, S. Irreversible adsorption erases the free surface effect on the T_g of supported films of poly (4-tert-butylstyrene. *ACS Macro Lett.* **2017**, *6*, 354−358.

(4) Ediger, M. D.; Forrest, J. Dynamics near free surfaces and the glass transition in thin polymer films: a view to the future. *Macromolecules* **2014**, *47*, 471−478.

(5) Napolitano, S.; Glynos, E.; Tito, N. B. Glass transition of polymers in bulk, confined geometries, and near interfaces. *Rep. Prog. Phys.* **2017**, *80*, No. 036602.

(6) Ellison, C. J.; Torkelson, J. M. The distribution of glass-transition temperatures in nanoscopically confined glass formers. *Nat. Mater.* **2003**, *2*, 695−700.

(7) Hanakata, P. Z.; Douglas, J. F.; Starr, F. W. Interfacial mobility scale determines the scale of collective motion and relaxation rate in polymer films. *Nat. Commun.* **2014**, *5*, No. 4163.

(8) Chowdhury, M.; Priestley, R. D. Discrete mobility on the surface of glasses. *Proc. Natl. Acad. Sci. U.S.A.* **2017**, *114*, 4854−4856.

(9) Napolitano, S. Irreversible adsorption of polymer melts and nanoconfinement effects. *Soft Matter* **2020**, *16*, 5348−5365.

(10) Schweizer, K. S.; Simmons, D. S. Progress towards a phenomenological picture and theoretical understanding of glassy dynamics and vitrification near interfaces and under nanoconfinement. *J. Chem. Phys.* **2019**, *151*, No. 240901.

(11) Hao, Z.; Ghanekarade, A.; Zhu, N.; Randazzo, K.; Kawaguchi, D.; Tanaka, K.; Wang, X.; Simmons, D. S.; Priestley, R. D.; Zuo, B. Mobility gradients yield rubbery surfaces on top of polymer glasses. *Nature* **2021**, *596*, 372−376.

(12) Koga, T.; Jiang, N.; Gin, P.; Endoh, M.; Narayanan, S.; Lurio, L.; Sinha, S. Impact of an irreversibly adsorbed layer on local viscosity of nanoconfined polymer melts. *Phys. Rev. Lett.* **2011**, *107*, No. 225901.

(13) Chowdhury, M.; Guo, Y.; Wang, Y.; Merling, W. L.; Mangalara, J. H.; Simmons, D. S.; Priestley, R. D. Spatially Distributed Rheological Properties in Confined Polymers by Noncontact Shear. *J. Phys. Chem. Lett.* **2017**, *8*, 1229−1234.

(14) Geng, K.; Katsumata, R.; Yu, X.; Ha, H.; Dulaney, A. R.; Ellison, C. J.; Tsui, O. K. Conflicting confinement effects on the T_g, diffusivity, and effective viscosity of polymer films: A case study with poly (isobutyl methacrylate) on silica and possible resolution. *Macromolecules* **2017**, *50*, 609−617.

(15) Priestley, R. D.; Ellison, C. J.; Broadbelt, L. J.; Torkelson, J. M. Structural relaxation of polymer glasses at surfaces, interfaces, and in between. *Science* **2005**, *309*, 456−459.

(16) Kumar, S. K.; Jimenez, A. M. Polymer adsorption−reversible or irreversible? *Soft Matter* **2020**, *16*, 5346−5347.

(17) Priestley, R. D.; Cangialosi, D.; Napolitano, S. On the equivalence between the thermodynamic and dynamic measurements of the glass transition in confined polymers. *J. Non-Cryst. Solids* **2015**, *407*, 288−295.

(18) Donth, E.-J. *The Glass Transition: Relaxation Dynamics in Liquids and Disordered Materials*; Springer: Berlin, 2013; Vol. *48*.

(19) Angell, C. A.; Ngai, K. L.; McKenna, G. B.; McMillan, P. F.; Martin, S. W. Relaxation in glassforming liquids and amorphous solids. *J. Appl. Phys.* **2000**, *88*, 3113−3157.

(20) Boucher, V. M.; Cangialosi, D.; Yin, H.; Schönhals, A.; Alegrá, A.; Colmenero, J. T_g depression and invariant segmental dynamics in polystyrene thin films. *Soft Matter* **2012**, *8*, 5119−5122.

(21) Zhang, C.; Boucher, V. M.; Cangialosi, D.; Priestley, R. D. Mobility and glass transition temperature of polymer nanospheres. *Polymer* **2013**, *54*, 230−235.

(22) Pye, J. E.; Roth, C. B. Two simultaneous mechanisms causing glass transition temperature reductions in high molecular weight freestanding polymer films as measured by transmission ellipsometry. *Phys. Rev. Lett.* **2011**, *107*, No. 235701.

(23) Glor, E. C.; Angrand, G. V.; Fakhraai, Z. Exploring the broadening and the existence of two glass transitions due to

competing interfacial effects in thin, supported polymer films. *J. Chem. Phys.* **2017**, *146*, No. 203330.
(24) Pradipkanti, L.; Chowdhury, M.; Satapathy, D. K. Stratification and two glass-like thermal transitions in aged polymer films. *Phys. Chem. Chem. Phys.* **2017**, *19*, 29263−29270.
(25) Zhang, Y.; Fakhraai, Z. Decoupling of surface diffusion and relaxation dynamics of molecular glasses. *Proc. Natl. Acad. Sci. U.S A.* **2017**, *114*, 4915−4919.
(26) Baglay, R. R.; Roth, C. B. Communication: Experimentally determined profile of local glass transition temperature across a glassy-rubbery polymer interface with a T_g difference of 80 K. *J. Chem. Phys.* **2015**, *143*, No. 111101.
(27) Monnier, X.; Cangialosi, D. Thermodynamic ultrastability of a polymer glass confined at the micrometer length scale. *Phys. Rev. Lett.* **2018**, *121*, No. 137801.
(28) Xu, Q.; Zhu, N.; Fang, H.; Wang, X.; Priestley, R. D.; Zuo, B. Decoupling Role of Film Thickness and Interfacial Effect on Polymer Thin Film Dynamics. *ACS Macro Lett.* **2021**, *10*, 1−8.
(29) Napolitano, S.; Cangialosi, D. Interfacial free volume and vitrification: Reduction in T_g in proximity of an adsorbing interface explained by the free volume holes diffusion model. *Macromolecules* **2013**, *46*, 8051−8053.
(30) Zha, H.; Wang, Q.; Wang, X.; Cangialosi, D.; Zuo, B. Enhanced Free Surface Mobility Facilitates the Release of Free-Volume Holes in Thin-Film Polymer Glasses. *Macromolecules* **2021**, *54*, 2022−2028.
(31) Burroughs, M. J.; Napolitano, S.; Cangialosi, D.; Priestley, R. D. Direct measurement of glass transition temperature in exposed and buried adsorbed polymer nanolayers. *Macromolecules* **2016**, *49*, 4647−4655.
(32) Bodiguel, H.; Fretigny, C. Reduced viscosity in thin polymer films. *Phys. Rev. Lett.* **2006**, *97*, No. 266105.
(33) Campbell, C. G.; Vogt, B. D. Examination of the influence of cooperative segmental dynamics on the glass transition and coefficient of thermal expansion in thin films probed using poly (n-alkyl methacrylate) s. *Polymer* **2007**, *48*, 7169−7175.
(34) Zhang, W.; Douglas, J. F.; Starr, F. W. Why we need to look beyond the glass transition temperature to characterize the dynamics of thin supported polymer films. *Proc. Natl. Acad. Sci. U.S.A.* **2018**, *115*, 5641−5646.
(35) Forrest, J. A.; Dalnoki-Veress, K. When does a glass transition temperature not signify a glass transition? *ACS Macro Lett.* **2014**, *3*, 310−314.
(36) Schawe, J. E.; Pogatscher, S. *Fast Scanning Calorimetry*, Springer, 2016; pp 3−80.
(37) Cangialosi, D.; Alegrá, A.; Colmenero, J. *Fast Scanning Calorimetry*, Springer, 2016; pp 403−431.
(38) Shoifet, E.; Schulz, G.; Schick, C. Temperature modulated differential scanning calorimetry−extension to high and low frequencies. *Thermochim. Acta* **2015**, *603*, 227−236.
(39) Perez-de Eulate, N. G.; Di Lisio, V.; Cangialosi, D. Glass transition and molecular dynamics in polystyrene nanospheres by fast scanning calorimetry. *ACS Macro Lett.* **2017**, *6*, 859−863.
(40) Badrinarayanan, P.; Zheng, W.; Li, Q.; Simon, S. L. The glass transition temperature versus the fictive temperature. *J. Non-Cryst. Solids* **2007**, *353*, 2603−2612.
(41) Moynihan, C. T.; Easteal, A. J.; De Bolt, M. A.; Tucker, J. Dependence of the fictive temperature of glass on cooling rate. *J. Am. Ceram. Soc.* **1976**, *59*, 12−16.
(42) Derjaguin, B.; Karassev, V. Viscosity studies of liquid boundary layers by the blow-off method. *Prog. Surf. Sci.* **1992**, *40*, 301−308.
(43) Scarpulla, M. A.; Mate, C. M.; Carter, M. D. Air shear driven flow of thin perfluoropolyether polymer films. *J. Chem. Phys.* **2003**, *118*, 3368−3375.
(44) Mate, C. M.; Marchon, B. Shear response of molecularly thin liquid films to an applied air stress. *Phys. Rev. Lett.* **2000**, *85*, 3902.
(45) Rivetti, M.; Salez, T.; Benzaquen, M.; Raphaël, E.; Bäumchen, O. Universal contact-line dynamics at the nanoscale. *Soft Matter* **2015**, *11*, 9247−9253.
(46) Chowdhury, M.; Al Akhrass, S.; Ziebert, F.; Reiter, G. Relaxing nonequilibrated polymers in thin films at temperatures slightly above the glass transition. *J. Polym. Sci., Part B: Polym. Phys.* **2017**, *55*, 515−523.
(47) Chandran, S.; Baschnagel, J.; Cangialosi, D.; Fukao, K.; Glynos, E.; Janssen, L. M.; Mueller, M.; Muthukumar, M.; Steiner, U.; Xu, J.; Napolitano, S.; Reiter, G. Processing pathways decide polymer properties at the molecular level. *Macromolecules* **2019**, *52*, 7146−7156.
(48) Priestley, R. D.; Mundra, M. K.; Barnett, N. J.; Broadbelt, L. J.; Torkelson, J. M. Effects of nanoscale confinement and interfaces on the glass transition temperatures of a series of poly (n-methacrylate) films. *Aust. J. Chem.* **2007**, *60*, 765−771.
(49) Song, Z.; White, R. P.; Lipson, J. E.; Napolitano, S. Experimental and Modeling Comparison of the Dynamics of Capped and Freestanding Poly (2-chlorostyrene) Films. *ACS Macro Lett.* **2022**, *11*, 91−95.
(50) Napolitano, S.; Pilleri, A.; Rolla, P.; Wubbenhorst, M. Unusual deviations from bulk behavior in ultrathin films of poly (tert-butylstyrene): Can dead layers induce a reduction of T_g? *ACS Nano* **2010**, *4*, 841−848.
(51) Schawe, J. E. K. Vitrification in a wide cooling rate range: The relations between cooling rate, relaxation time, transition width, and fragility. *J. Chem. Phys.* **2014**, *141*, No. 184905.
(52) Panagopoulou, A.; Napolitano, S. Irreversible adsorption governs the equilibration of thin polymer films. *Phys. Rev. Lett.* **2017**, *119*, No. 097801.
(53) Saito, Y.; Sasaki, N.; Komatsu, T. Molecular dynamics simulation for lubricant shear properties during heating. *IEEE Trans. Magn.* **2012**, *48*, 2009−2015.
(54) George, G.; Kriuchevskyi, I.; Meyer, H.; Baschnagel, J.; Wittmer, J. Shear-stress relaxation in free-standing polymer films. *Phys. Rev. E* **2018**, *98*, No. 062502.

https://doi.org/10.1021/acspolymersau.2c00010
ACS Polym. Au 2022, 2, 333−340